

Nonselective Adsorption of Block Copolymers and the Effect of Block Incompatibility

Henri D. Bijsterbosch,* Martien A. Cohen Stuart, and Gerard J. Fleer

Department of Physical and Colloid Chemistry, Wageningen Agricultural University, Dreijenplein 6, 6703 HB Wageningen, The Netherlands

Peter van Caeter and Eric J. Goethals

Department of Organic Chemistry, Polymer Division, University of Ghent, Krijgslaan 281 S4-bis, 9000 Ghent, Belgium

Received December 20, 1996; Revised Manuscript Received April 9, 1998

ABSTRACT: The adsorbed amount and the hydrodynamic layer thickness of two series of block copolymers and the corresponding homopolymers on silica were determined. We used diblock copolymers of poly(vinyl methyl ether) and poly(2-ethyl-2-oxazoline) and tri- and diblock copolymers of poly(2-methyl-2-oxazoline) and poly(ethylene oxide). The diblock copolymers of poly(ethylene oxide) and poly(2-methyl-2-oxazoline) were obtained by polymerization of 2-methyl-2-oxazoline initiated by the tosylate of poly(ethylene glycol) monomethyl ether. The difference between the adsorption energies of the segments is found to be small: the block copolymer adsorption is nonselective. The adsorbed amount as a function of block copolymer composition shows a maximum at a composition where the longest block is also the strongest adsorbing block. The adsorbed amounts and the layer thicknesses are relatively low. Similar results are obtained with numerical self-consistent field calculations for nonselective adsorption for the case when the different blocks are incompatible. The typical anchor–buoy structure of the adsorbed layer is maintained, albeit less explicit than that found for selective adsorption.

Introduction

Polymers play an important role in many industrial and natural processes and in various applications. One of the relevant features is their interfacial behavior. It has long been recognized that polymers can change the properties of colloidal dispersions. For example, they can be used for controlled flocculation or, conversely, for steric stabilization. Much experimental and theoretical attention has been paid to the different aspects of polymer adsorption; for a detailed survey, we refer to recent reviews.^{1,2}

In this paper we consider the adsorption of block copolymers, in which the various kinds of segments are distributed in blocks along the chain. Because of their dualistic character, block copolymers may be amphiphilic; they behave very differently from homopolymers.

Much attention has been paid to the adsorption of block copolymers in which one of the blocks does adsorb to a surface whereas the other block does not have any affinity for that surface; this situation may be referred to as *surface-selectivity*. From these theoretical^{3–5} and experimental^{6–11} studies we now have a rather complete picture of the behavior of block copolymers at interfaces. Upon adsorption of diblock copolymers, the adsorbing *anchor* block will form a relatively thin layer on the surface, whereas the nonadsorbing blocks form a rather dilute and extended *buoy* layer. The relative length of the blocks is of great importance for the structure of the polymer layer. When the adsorbing anchor block is long, the adsorption is limited by saturation of the anchoring layer; the lateral repulsion between the buoy blocks is then weak compared to the adsorption energy. Decreasing the relative length of the anchor will enhance the adsorbed amount because the total mass of adsorbed anchor segments remains more or less con-

stant and the relative contribution of the buoy segments to the adsorbed amount increases. This behavior is sometimes denoted the *anchor regime*.

When the relative length of the anchoring block is further decreased, we find a crossover to the *buoy regime*: the lateral repulsion between the buoy blocks is now more important than the gain in adsorption energy of the anchor blocks, and the total adsorbed amount decreases with decreasing anchor length. In Figure 1a this scenario is illustrated by plotting the adsorbed amount (θ^a) as a function of the block copolymer composition for different total chain lengths N . Figure 1b gives the volume fraction profiles ($\varphi(z)$) of the two blocks in the maximum, for $N = 100$. These figures were calculated with a self-consistent-field theory,⁵ but the same qualitative results are obtained with other theories.³ The total length clearly affects the adsorption behavior of the block copolymer. With increasing length the maximum becomes more pronounced and shifts to a lower fraction v_A of anchor segments A. For the longer chains a smaller *fraction* of anchor segment is needed to give long enough anchor blocks to secure attachment. From the volume fraction profiles (Figure 1b) it is seen that almost all anchor segments can be found in the first few layers next to the surface. The buoy segments, on the other hand, avoid contact with the surface and form an extended layer. This extended layer, in which the polymers are stretched away from the surface,¹² can be important for the steric stabilization of colloidal dispersions.¹³

Adsorption of block copolymers can take place from a solvent that is either nonselective or selective. Figure 1 was calculated for a nonselective solvent in which both blocks are equally soluble. In a selective solvent one of the blocks can be insoluble and the block copolymers may form micelles in solution. The qualitative features

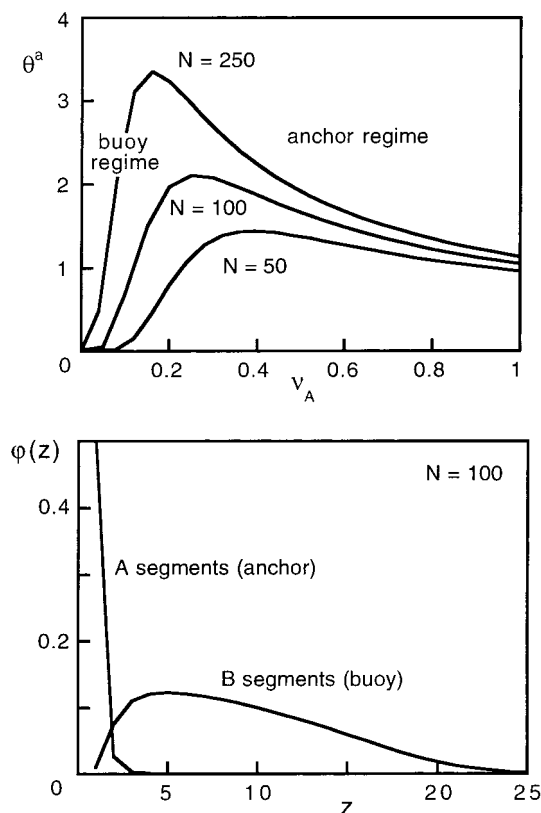


Figure 1. The adsorbed amount (θ^a) as a function of block copolymer composition for different chain lengths, ν_A is the fraction A segments of the total number of segments (a), and the volume fraction profiles ($\phi(z)$) of the two blocks in the maximum for $N = 100$, z is the distance to the surface in number of lattice layers (b). Adsorption energy of the A segments, χ_{sA} , is $2kT$, all other interaction parameters are zero. Calculations were made with the help of a SCF theory using a cubic lattice.

for a nonselective solvent and for a selective solvent in which the anchor blocks do not dissolve are expected to be roughly the same (i.e., as in Figure 1).^{14,15} However, when in a selective solvent the soluble block (i.e., the micellar corona) does adsorb, it is very likely that associative adsorption occurs and that micellar structures accumulate at the surface.^{15–17} This scenario can be very complex, and the kinetic parameters probably influence the final conformation of the adsorbed polymer.^{18–20} We have to keep in mind that the picture as given in Figure 1 is for a system at equilibrium. In natural processes and in certain experiments such equilibrium conditions may not be attained, especially so when the solvent is selective.

Above, we sketched the situation for *selective adsorption*, where one of the blocks is adsorbing and the other has no affinity for the surface. In real systems, however, often both blocks of a diblock copolymer can adsorb to a surface. We may denote this situation as *nonselective adsorption*. The properties of the adsorbed layer are now determined by the competition for anchoring sites between the two blocks. So far, this competition between two adsorbing blocks within one polymer has not been studied in detail. In a few papers this aspect has been considered,^{5,21} but when the difference between the adsorption energies of the two segment types is relatively high, the behavior is not greatly different from that of selective adsorption. In this paper we describe the adsorption of two different sets of block copolymers

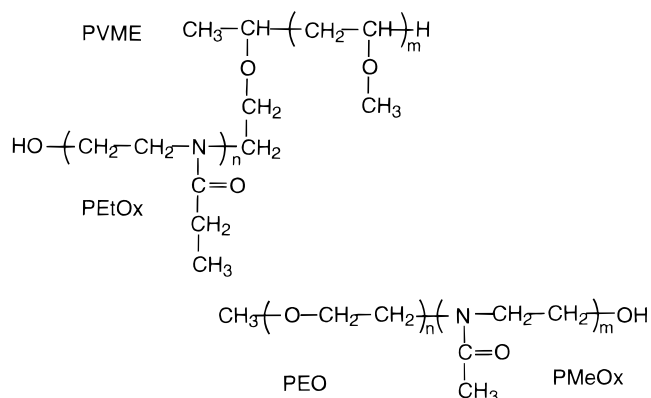


Figure 2. Structural formulas of some of the polymers used. The PMeOx living end group is not specially treated, in the aqueous environment, the ring structure is probably opened and end functionalized with a hydroxyl group.

at the silica–water interface. For the two types of segments in these copolymers, the difference in adsorption energy for the surface turned out to be rather low. We used a series of diblock copolymers of poly(vinyl methyl ether) and poly(2-ethyl-2-oxazoline) and a series of diblock copolymers of poly(ethylene oxide) and poly(2-methyl-2-oxazoline). We measured the adsorbed amount with optical reflectometry as well as the hydrodynamic layer thickness with dynamic light scattering. To get a complete picture, also numerical self-consistent field calculations were carried out. In this theoretical modeling special attention is paid to the effect of incompatibility of the two blocks within the polymer. So far, this aspect has hardly received any attention in the literature.

Experimental Section

Materials. We used four types of homopolymers: poly(vinyl methyl ether) (PVME), poly(2-methyl-2-oxazoline) (PMeOx), poly(2-ethyl-2-oxazoline) (PEtOx), and poly(ethylene oxide) (PEO). The block copolymers were three PVME–PEtOx and three PMeOx–PEO diblock copolymers. The structural formulas of typical representatives of these polymers are given in Figure 2. The PEtOx and PMeOx homopolymers were synthesized and kindly given to us by F. Derks (DSM, The Netherlands). The PVME homopolymer is a commercial product (Scientific Polymer Science), as is PEO (Polymer Laboratories). The block copolymers of PVME and PEtOx were synthesized²² and kindly made available by Dr. J. Riffle (Virginia State University). Triblock copolymers of PMeOx and PEO can be synthesized by cationic polymerization of the oxazoline block, starting with a bifunctional PEO homopolymer macroinitiator.²³ The synthesis of the diblock copolymers of PMeOx and PEO is different because we had to start with a monofunctional PEO. As this synthesis has not been described earlier in the literature, we give the procedure in the next section.

Some of the characteristics of the polymer samples used are given in Table 1. The number in the sample name for the block copolymers gives the percentage of the first block in the total molar mass, for which we choose the block with the highest affinity for the surface. As we shall see, PVME adsorbs more strongly than PEtOx, and PMeOx adsorbs more strongly than PEO. The commercial homopolymer PVME has a high polydispersity ($M_w/M_n = 2.1$). All the other polymers were synthesized by living ionic polymerization, and therefore the molar mass distributions are relatively narrow. The value of the refractive index increment dn/dc for the PEO homopolymer was taken from the literature;²⁴ the values for the other homopolymers were obtained with the group contribution method as described by van Krevelen.²⁵ The refractive index

Table 1. Molecular (block) Structure, Molar Mass, and Refractive Index Increment of the Polymers Used; the Molar Mass of PVME-PEtOx 17 Has Not Been Determined, Indicated Is the Target Molar Mass during Synthesis

sample	M_w , kg mol ⁻¹	no. of monomers	dn/dc , cm ³ g ⁻¹
PVME	99	1650	0.146
PVME-PEtOx 63	15.7-9.2	260-91	0.152
PVME-PEtOx 42	7.5-10.3	125-102	0.155
PVME-PEtOx 17	2.0-8.0	33-79	0.158
PEtOx	6.0	59	0.161
PEtOx	55	540	0.161
PMeOx	6.0	69	0.160
PMeOx-PEO 89	5.8-0.75	67-17	0.157
PMeOx-PEO 67	4.3-2.1	49-47	0.152
PMeOx-PEO 17	1.0-5.0	11-114	0.140
PEO	7.1	161	0.136

increments for the block copolymers were calculated from the homopolymer values, assuming additivity of the refractive index. Polymer solutions were made up by dissolving the dry material in deionized water, and were stored in a refrigerator. Measurements of the adsorbed amount and the hydrodynamic thickness were performed at room temperature.

Synthesis of PMeOx and PEO Diblock Copolymers. Commercial poly(ethylene glycol) monomethyl ether (PEO monomethyl ether) ($M_w = 750, 2000,$ and 5000 from Fluka) was dried in vacuo at $60\text{ }^\circ\text{C}$ in the presence of phosphorus pentoxide for 24 h. Benzene was dried over sodium wire and distilled under nitrogen. Tosyl chloride was purified by sublimation under reduced pressure. Acetonitrile was dried over CaH_2 and distilled under nitrogen. 2-Methyl-2-oxazoline was purified by distillation over KOH pellets and CaH_2 under nitrogen. *n*-Butyllithium (1.6 M solution in hexane from Aldrich) was used as received.

Poly(ethylene glycol) monomethyl ether was converted to the corresponding tosylate ester in analogy to a reported procedure for the synthesis of α,ω -ditosylated PEO.²⁶ First, the alcohol end group was converted into the lithium alcoholate with a stoichiometric amount of *n*-butyllithium (*n*-BuLi) in benzene, followed by the reaction with tosyl chloride; the reaction scheme is given in the top line of Figure 3. As a typical example of the synthesis of PEO monotosylate (TsPEO), the preparation of a TsPEO sample with a molar mass of 2100 g mol^{-1} is described. A solution of 30 g of PEO monomethyl ether ($M_w = 2000\text{ g mol}^{-1}$) in 300 mL of benzene was cooled to $5\text{ }^\circ\text{C}$ under nitrogen. Under stirring, 10.3 mL of a 1.6 M solution of *n*-butyllithium was added rapidly followed by 3.43 g of tosyl chloride, dissolved in 30 mL of benzene. The resulting mixture was stirred overnight at room temperature. The lithium chloride precipitate was filtered off, the filtrate evaporated in vacuo until dryness, and the residue dissolved in 40 mL of dry ethanol at room temperature. The solution was cooled to $-18\text{ }^\circ\text{C}$ for 1 h and the resulting precipitate was filtered off under dry nitrogen on a cooled glass filter. After the product was dried *in vacuo* at $60\text{ }^\circ\text{C}$ in the presence of phosphorus pentoxide for 24 h, 30.9 g of TsPEO was obtained. Three samples were synthesized, with molar masses of $740, 2100,$ and 5200 g mol^{-1} , respectively; all samples have an end group functionality of 1.0. The molar masses and the end group functionalities were determined by the integral ratio of the tosyl to ethylene peaks in the $500\text{ MHz } ^1\text{H NMR}$ spectra in CDCl_3 . The polydispersity index M_w/M_n , measured by GPC, using a PL-Gel 10 MIX Å column, CHCl_3 as eluent, and calibration on PS standards, was 1.1 for all three samples.

The monofunctional TsPEO was used as a macro initiator for the polymerization of 2-methyl-2-oxazoline (MeOx), as indicated in the bottom lines of Figure 3. In this way AB block copolymers consisting of an A-block of PEO and a B-block of poly(2-methyl-2-oxazoline) (PMeOx) were obtained in analogy to a reported procedure for the synthesis of analogous ABA block copolymers of the same block segments.²³ As a typical example, the preparation of PMeOx-PEO 67 is described. TsPEO with $M_w = 2000\text{ g mol}^{-1}$ ($3.3\text{ g}, 1.5\text{ mmol}$) was

transferred into a 100 mL "heavy wall glass tube" containing 30 mL of acetonitrile under nitrogen. MeOx ($6.7\text{ mL}, 79\text{ mmol}$) was added, and the tube was sealed and heated to $90\text{ }^\circ\text{C}$. After 20 h , the reaction mixture was cooled and poured into 2 L of diethyl ether. The precipitated block copolymer was isolated by decantation and purified by reprecipitation from chloroform solution in diethyl ether. The pale yellow solid was dried in vacuo at $60\text{ }^\circ\text{C}$ in the presence of phosphorus pentoxide for 24 h . The yield was 9.5 g . In this way the three PMeOx-PEO diblock copolymer samples indicated in Table 1 were synthesized. The molar masses were determined by the integral ratio in the $500\text{ MHz } ^1\text{H NMR}$ spectra in CDCl_3 . The ratio M_w/M_n was 1.2 for all three samples, as measured by GPC, using a Waters Styragel HT 10^3 Å (10) + 10^4 Å (10) column, *N*-methylpyrrolidone ($80\text{ }^\circ\text{C}$) as eluent, and calibration on PS standards. The yield, calculated as %-conversion of the MeOx polymerization, was between 95 and 97%. Comparison of the GPC analysis of one of the AB block copolymers with that of the original TsPEO prepolymer showed that a considerable increase in the molar mass had occurred and that the reaction mixture contained no unreacted macroinitiator.

Reflectometry. The adsorbed amounts of polymer were measured in a reflectometer with a stagnation-point flow cell as described in detail by Dijt et al.²⁷ Here we give only a brief summary. An oxidized silicon substrate can be placed in the stagnation point of the cell. Upon adsorption of polymer onto this substrate the reflectance of a polarized laser beam is changed. The change in signal is proportional to the adsorbed amount Γ . The proportionality factor can easily be calculated from a suitable optical model. The sensitivity of the method depends, among other things, on the thickness of the oxide layer d_{ox} , on the refractive indices of silicon, silica, and solution (n_{Si} , n_{ox} , and n_s , respectively), and on the refractive index increment dn/dc of the polymer in solution. The values of dn/dc are indicated in Table 1.

Macroscopically flat silicon wafers from Aurel GmbH (Germany) were used. By thermal oxidation, we obtained an SiO_2 layer with a thickness of about 110 nm . Strips cut from this wafer were cleaned by oxidation by UV-ozone, and they could be cleaned and reused many times.

Dynamic Light Scattering. The hydrodynamic thickness of the adsorbed polymer layer was measured by dynamic light scattering. The radius of a colloidal silica particle covered with polymer was compared to that of a bare particle, and the difference was taken as the hydrodynamic thickness of the adsorbed polymer layer. We used a colloidal Ludox silica with a hydrodynamic diameter of 39 nm , purchased from Du Pont.

Calculations. Scaling theories^{3,14} and self-consistent mean field theories (SCF)^{5,15} have proven to be very useful in describing block copolymer adsorption. Here we used a numerical SCF method first developed by Scheutjens and Fleer for homopolymer adsorption^{1,28,29} and later adapted for block copolymer adsorption by Evers et al.⁵ To investigate whether there is an effect of the chain stiffness, calculations for both flexible and stiff polymers were done. In the latter case a second-order Markov approximation³⁰ was used. In the calculations the composition of an AB block copolymer was varied by changing the numbers of A and B segments, keeping the total number of segments constant. We chose a rather small number of segments ($N = 100$) in order to make it possible to compare the results qualitatively with the experimental system, in which we used block copolymers with a rather low molar mass. The calculations were done on a cubic lattice.

Results and Discussion

Homopolymer Adsorption. In reflectometry experiments the adsorbed amount is measured as a function of time. This gives a good opportunity to study the kinetics of polymer adsorption. It is assumed that when the variation in the signal has the same order of magnitude as that of the baseline drift, the system is at equilibrium. Of course, this may not be generally true because in some systems equilibrium may only be

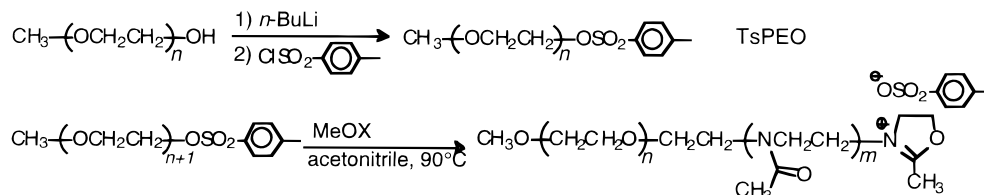


Figure 3. Reaction scheme for the synthesis of diblock copolymers of PEO and PMeOx. The top line gives the conversion of poly(ethylene glycol) monomethyl ether to the corresponding tosylate ester. This ester is used as a macroinitiator for the polymerization of 2-methyl-2-oxazoline, as indicated in the bottom lines.

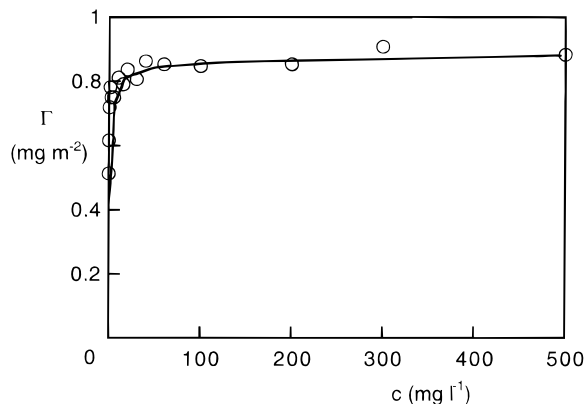


Figure 4. Adsorption isotherm of PVME on silica at pH = 6, as measured by reflectometry.

obtained on much longer time scales than those needed for reflectometry (typically on the order of minutes, with a maximum of a few hours). However, for our experimental system the above assumption is expected to hold, since we are dealing with small, rather flexible polymers which do not form any micellar structure in solution, as evidenced by dynamic light scattering on the polymer solutions. For monodisperse homopolymer solutions of PEtOx, PMeOx, and PEO at concentrations of 10 mg L⁻¹, a plateau in the adsorbed amount is reached within 1 min. We also find a very sharp transition from a linear (transport-limited) regime to saturation, in agreement with other results for flexible polymers.²⁷ For the 10 mg L⁻¹ solution of polydisperse PVME the adsorption curve as a function of time is different. The slope of the linear part is lower due to the lower diffusion coefficient of this polymer, which has a much higher molar mass than the other polymers used in these experiments. The transition to saturation is less sharp. This is a general feature of polydisperse polymers.^{1,27} In the initial linear part of the curve, all chain lengths present in the polydisperse polymer solution contribute to the adsorption. However, the plateau values of the polymers with different molar mass are not equal, the short polymers having a lower adsorbed amount in the plateau. The contribution of the short chains to the adsorption can never exceed the plateau of these short polymers, whereas the longer chains can reach a higher level. Hence, the short chains are displaced by the longer chains, and the adsorption curve of a polydisperse polymer solution is thus more rounded than that of a monodisperse sample.

For two of the homopolymers we measured the final adsorbed amounts after saturation on silica as a function of the polymer concentration. The resulting adsorption isotherms, for PVME and PEtOx, respectively, are given in Figures 4 and 5.

The error in the result of one reflectometry experiment can be rather large, up to 10% deviation from the

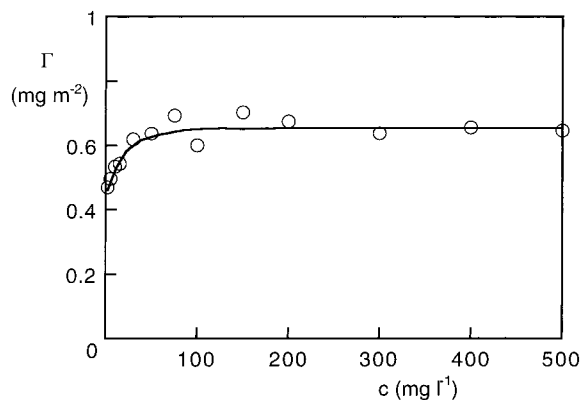


Figure 5. Adsorption isotherm of PEtOx on silica at pH = 6, as measured by reflectometry.

average. It is therefore necessary to do many experiments to obtain accurate results. Although the measurements for the adsorption isotherms were only done twice, the general trends are clear. The high-affinity isotherms we see in Figures 4 and 5 are characteristic for polymers. Only for very low polymer concentrations (less than 2 mg L⁻¹) is the equilibrium adsorbed amount lower than that in the plateau of the isotherm. This feature is not necessarily unambiguous, because reflectometry is less accurate at extremely low concentrations due to the long time needed for one measurement in our experimental setup.

We did not measure a full adsorption isotherm for PEO, because in this case literature data³¹ are available. PEO gives also a high affinity isotherm³¹ with a plateau starting well below 10 mg L⁻¹. We may assume that the same holds for PMeOx. Hence, a polymer concentration of 10 mg L⁻¹, which we used as the standard in the experiment, may be assumed to be sufficient to reach the plateau of the adsorption isotherm. The adsorbed amounts at this concentration are 0.78, 0.56, 0.53, and 0.36 mg m⁻² for PVME, PEtOx, PMeOx and PEO, respectively. Dijt et al.²⁷ found for the same PEO sample with the same technique an adsorbed amount of 0.41 mg m⁻², which agrees, within experimental error, with our results. Chen et al.³² used a solution depletion method to determine the adsorption isotherms for a series of PEtOx with different molar mass on colloidal silica. Our result for PEtOx with $M_w = 6000$ fits well in their results, even though we used a quite different technique and also the surface is slightly different.

The adsorption of PEO and PEtOx presumably proceeds by hydrogen bonding of the ether or carbonyl oxygen with surface silanol groups.³¹ The adsorption of the other polymers is also likely to be driven by hydrogen bonding since they all have an oxygen which can donate an electron pair for a hydrogen bond with the silica surface. Chen et al.³² found that the segmen-

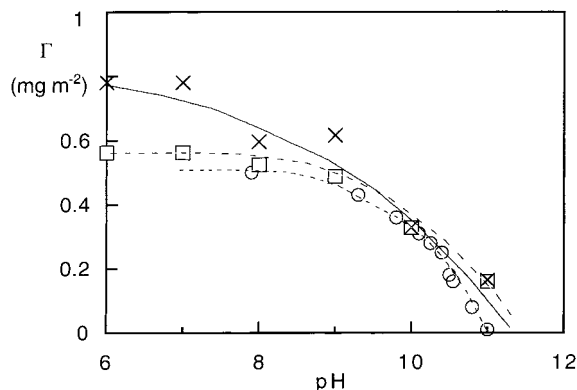


Figure 6. Adsorption of PVME (squares) and PETox (triangles) as a function of pH, as measured by reflectometry on a flat silica surface. The results found by Van der Beek et al. for PEO on a colloidal silica have been included (circles).

tal adsorption energy of PETox on silica was $5.1 kT$ in water. One way to check the role of the hydrogen bond is to measure the adsorption as a function of the pH of the solution; at high pH there are less silanols so that hydrogen bonding is impeded. For PVME and PETox the results are given in Figure 6. Data by Van der Beek et al.³¹ for PEO on colloidal silica have been included in this figure.

The shape of the curves is the same for the three homopolymers. The adsorbed amount is almost constant up to about neutral pH. When the polymer solution is made basic desorption occurs. At high pH (above pH around 11) no adsorption is found at all. As discussed by Van der Beek, the OH ions in solution act as a displacer for the polymers since they deprotonate the silanols. Increasing the concentration of these ions, i.e., increasing the pH, lowers the effective adsorption energy of the polymers because the oxygens are no longer able to form hydrogen bonds with the surface. The adsorbed amount drops to zero around pH = 11. It can be seen from Figure 6 that a slightly higher pH is needed to displace all PVME and PETox than to displace all PEO. It is tempting to ascribe this to a higher adsorption energy for PVME and PETox. However, we have to be careful because the surfaces were different: the adsorption of PEO was measured on dispersed colloidal silica particles,³¹ whereas we measured the adsorption of PVME and PETox on a flat silica wafer. It is conceivable that there might be slight differences in properties between these surfaces.

All homopolymers adsorb on silica, and the difference in segmental adsorption energy is probably not high, as can be deduced from Figure 6. To assess which of the two blocks within one block copolymer has the higher segmental adsorption energy, we measured the adsorption from a mixture of two homopolymers and in sequential adsorption experiments. Even a small difference in adsorption energy between the segments could be enough to obtain a significant preferential adsorption of the more strongly adsorbing polymer, due to the cooperative nature of polymer adsorption: a small difference in adsorption energy per segment will nevertheless give a large difference per chain. Measurement of sequential adsorption or adsorption from a mixture can therefore indicate which polymer has the highest adsorption energy.¹

Preferential adsorption is also favored for longer chains, but the effects of adsorption energy are stronger than those of chain length. Theoretical calculations

show that displacement for chains of equal length is already effective for Δu_{ads} of order $0.01-0.1 kT$. These values become larger as the length N_D of the displacing chains becomes shorter, roughly proportionally to N_D^{-1} . We first found that in a mixture of PVME and PETox the adsorbed amount at saturation is the same as obtained for the isolated PVME solution. This suggests that no PETox adsorbs from the mixture, and it would indicate that the adsorption energy of PVME on silica is higher than that for PETox. This finding was confirmed by sequential measurements in which one of the polymers was adsorbed until a plateau was reached and then a solution of the second polymer was brought into contact with the surface. The height of the resulting adsorption plateau is determined by the polymer with the highest adsorption energy, i.e., PVME in a sequential adsorption experiment of PVME followed by PETox or reverse.

However, PVME has a molar mass that is an order of magnitude higher than that of PETox. It is possible that the adsorption energy of PETox is slightly higher than that of PVME but that the longer chain adsorbs preferentially because it loses less translational entropy (per unit of mass). We therefore repeated the experiments with two homopolymer samples which had a more similar molar mass: PVME with $M_w = 99\,000$ and PETox with $M_w = 50\,000$ (Polysciences Inc.). With reflectometry we found equal plateau adsorbed amounts for these two polymers. Hence, this measurement cannot give information on adsorption preference for this pair of polymers. We therefore decided to measure the difference in uptake of either polymer by particles of colloidal silica, by analyzing the supernatant solution. Thus, we compared the adsorbed amount of PETox onto a silica dispersion obtained from a pure PETox solution with that from a mixed solution with equal amounts of PETox and PVME. It turned out that the adsorbed amount of PETox from the mixture was four times lower than that from the pure PETox solution. This indicates that a large part of the silica surface is occupied by PVME. We also performed a sequential experiment in order to determine whether PVME can displace an already adsorbed layer of PETox. In this experiment, we adsorbed PETox onto the silica particles and then removed all remaining PETox from the solution. We then added a PVME solution with the same initial concentration as PETox. It appeared that after some time about 60% of the PETox had been displaced by PVME. Since the difference in molar mass between the samples is only a factor of 2, it is very unlikely that this can account for the adsorption preference of PVME. Hence, our observations strongly support the view that PVME adsorbs more strongly than PETox; i.e., the segmental adsorption energy of PVME is higher than that of PETox. The experiments also show that the difference is minor. One may wonder whether this result (obtained for a colloidal silica dispersion) may be extended to a macroscopically flat silica surface. There might be small differences between both surfaces and the adsorption energies of both polymers might thus be different for the two surfaces. However, both polymers adsorb via the same mechanism (hydrogen bonding), and a change in surface properties will thus probably affect the segmental adsorption energies of both polymers in the same way and to the same extent.

For the other two homopolymers we also determined which of the two had the highest adsorption energy. In

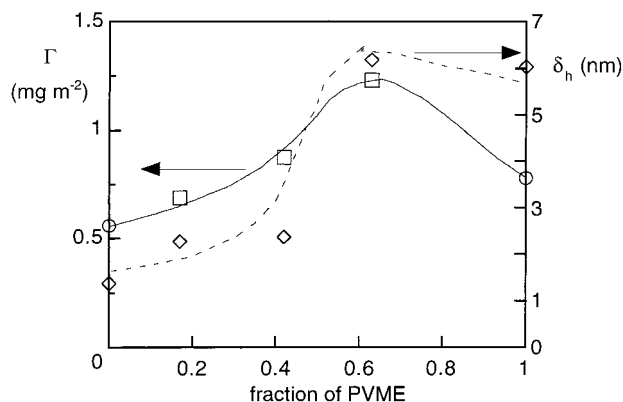


Figure 7. Adsorbed amount Γ (full line) of PVME-PEtOx diblock copolymers (squares) on silica as a function of polymer composition. The results for the homopolymers (circles) have been included. For all samples the hydrodynamic layer thickness δ_h on dispersed silica particles as measured by dynamic light scattering is also indicated (diamonds, dashed line).

this case it could be determined unambiguously from reflectometry data that the adsorption energy of PMeOx is higher than that of PEO. In this mixture the molar masses were comparable (6000 and 7100, respectively) and the preference was very clear. This finding was again confirmed by sequential measurements where one of the polymers was first adsorbed until a plateau was reached after which a solution of the second polymer was brought into contact with the surface. The height of the resulting adsorption plateau is determined by the polymer with the highest adsorption energy, i.e., PMeOx in a sequential adsorption experiment of PEO followed by PMeOx or reverse.

Block Copolymer Adsorption. From the homopolymer results it was concluded that PVME has a higher adsorption energy than PEtOx (but that the difference is small) and that PMeOx adsorbs more strongly than PEO. To see what the consequences are for the adsorption of diblock copolymers composed of these two blocks, we measured the adsorbed amount of these block copolymers.

Figure 7 gives the adsorbed amount on silica as a function of the composition of the PVME-PEtOx polymer. All measurements were repeated several times, and here we give only the average results. The circles correspond to the homopolymers (PEtOx on the left and PVME to the right), and the squares to the copolymers are as given in Table 1. For the block copolymers the adsorption is clearly enhanced compared to the values for the homopolymers, even though the molar mass of the homopolymer PVME is much higher than that of the block copolymers. Surprisingly, the position of the maximum is found at the side of the strongest adsorbing block: at this maximum the strongest adsorbing block is also the longest one. This is completely different from the situation sketched in Figure 1 for selective adsorption, where the maximum is found at a composition where the adsorbing block is smaller than the nonadsorbing block. In part, this could be due to the difference in chain length between the various samples. As can be seen from Table 1, the total mass of the PVME-PEtOx diblocks increases systematically in the direction of increasing ν_{PVME} , namely 6, 10, 18, and 25 kg/mol, respectively. As is clear from Figure 1, such a set of polymers would give a theoretical curve for which the maximum is not as pronounced as for a set of equally long polymers, and the maximum will be somewhat

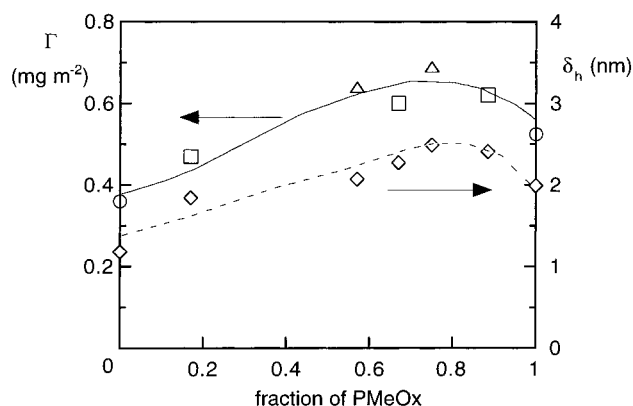


Figure 8. Adsorbed amount Γ (full line) of PMeOx-PEO diblock (squares) and triblock (triangles) copolymers on silica as a function of polymer composition. The results for the homopolymers (circles) have been included. For all samples the hydrodynamic layer thickness δ_h on dispersed silica particles as measured by dynamic light scattering is also indicated (diamonds, dashed line).

shifted toward higher ν_A . Nevertheless, the very clear maximum at $\nu_{PVME} = 0.6$ is not entirely explained by this chain length effect. We shall analyze this further in the section Comparison with Theory.

For the set of block copolymers consisting of PMeOx and PEO blocks, the former has the highest segmental adsorption energy. Here, the various samples have approximately equal molar masses. Results for this system are plotted in Figure 8. We see, as for PVME-PEtOx block copolymers, that the adsorbed amount for the block copolymers is higher than for the homopolymers. The maximum in the adsorbed amount is found at a high PMeOx fraction: again the strongest adsorbing block is also the longest one at the maximum, as in Figure 7. The maximum is not as pronounced as in Figure 7.

Hydrodynamic Layer Thickness. In Figures 7 and 8, the hydrodynamic thicknesses of PVME-PEtOx and PMeOx-PEO polymer layers, respectively, are also included. These layer thicknesses are less accurate than the adsorbed amounts, because although we did not observe flocculation of the colloidal silica dispersion, it cannot be completely ruled out. Hence, the results in Figures 7 and 8 give an upper limit of the hydrodynamic layer thickness.

The layer thicknesses are in agreement to what could be expected regarding the adsorbed amount and the molar mass. The PVME homopolymer, which has a rather high molar mass of 99 000 g mol⁻¹, gives a thickness of about 6.0 nm, a value comparable with the one found for PEO with the same molar mass.³¹ The other adsorbed homopolymers have very small layer thicknesses, as expected for these rather short polymers. The hydrodynamic thickness of the adsorbed block copolymers is higher than that of the homopolymers. The overall shape of the curves for the thickness and the adsorbed amount is very similar. In both Figures 7 and 8, a maximum for the layer thickness is seen at a polymer composition in which the strongest adsorbing block is also the longest one. Polymer PVME-PEtOx 63, the diblock copolymer of PVME and PEtOx which gave the highest adsorbed amount, also has the thickest adsorbed layer (6.2 nm). This is only slightly above the value of PVME homopolymer but the molar mass of the latter is considerably higher.

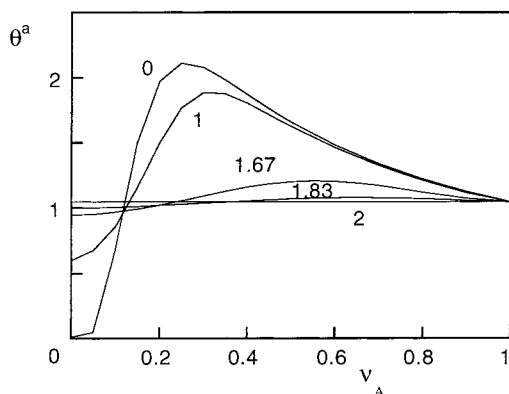


Figure 9. SCF calculations of the adsorbed amounts θ^a (expressed in equivalent monolayers) as a function of the fraction ν_A , for fully compatible blocks and an athermal solvent. Parameters: $\chi_{sA} = 2$, χ_{sB} is indicated, other χ -parameters are zero, and $N = 100$.

We summarize the experimental finding as follows. The block copolymers show a higher adsorbed amount and a higher hydrodynamic thickness as compared to the homopolymers of similar molar mass. However, the effects are not as pronounced as found for selectively adsorbed block copolymers, which is probably related to the small difference in adsorption energies. Nevertheless, this kind of block copolymers is promising for the steric stabilization of an aqueous dispersion, especially when fast equilibration is needed: these block copolymers do not have a kinetic barrier, since water is a nonselective solvent for these polymers so that no micelles are formed.

Comparison with Theory. In our experiments we found a maximum for the adsorbed amount and the layer thickness as a function of the block copolymer composition. In this maximum, the strongest adsorbing block is also the longest one, which differs from the theoretical curve given in Figure 1. In this figure, we showed results for adsorbing A segments and nonadsorbing B segments in an athermal solvent. In our experimental system both blocks have a relatively high adsorption energy for the surface, and the interaction parameters between solvent and polymer and between the two blocks (block compatibility) may not be zero. In this section we try to find out whether SCF theory, taking these effects into account, can offer some help in interpreting the experimental findings.

We first consider the adsorption of an AB diblock copolymer from a nonselective, in this case athermal solvent, as described earlier by Evers et al.⁵ We assigned a constant adsorption energy ($2kT$) to the A segments and increased the adsorption energy of the B segments from zero to $2kT$. In the latter case there is no difference between the blocks and the copolymer behaves like a homopolymer for all compositions. Figure 9 gives the adsorbed amount θ as a function of the fraction ν_A of A segments, where ν_A is defined as $\nu_A = N_A/N$, with $N = N_A + N_B = 100$.

For selective adsorption ($\chi_{sB} = 0$) we find the same maximum in the adsorbed amount as in Figure 1, i.e., at relatively low ν_A . When the adsorption energy of the B segments is increased, the maximum becomes less pronounced and shifts to higher ν_A . More importantly, for small differences in adsorption energy the maximum is found at a composition where the A block is longer than the B block. Obviously, the maximum disappears

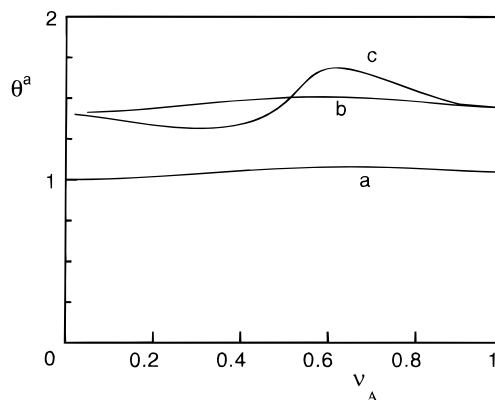


Figure 10. SCF calculations of the adsorbed amounts θ^a (expressed in equivalent monolayers) as a function of the fraction ν_A , for fully compatible block (a and b) or incompatible blocks (c) from a poorer solvent. Parameters: $\chi_{sA} = 2$, $\chi_{sB} = 1.83$, $N = 100$, for curve a, $\chi_{AO} = \chi_{BO} = \chi_{AB} = 0$, for curve b, $\chi_{AO} = \chi_{BO} = 0.45$ and $\chi_{AB} = 0$, and for curve c, $\chi_{AO} = \chi_{BO} = \chi_{AB} = 0.45$.

when there is no difference in adsorption energy ($\chi_{sB} = 2$).

By assigning an adsorption energy to the B segments, we introduce competition between the A and B segments. The total adsorbed amount is determined by the balance between the gain in adsorption energy and the loss in translational and configurational entropy of the adsorbing chains. When the surface is not yet saturated with block copolymer, free polymers from the solution can adsorb with their A block at the cost of translational entropy of that polymer. When the B segments have also an adsorption energy, some of the B segments of a chain already adsorbed by its A segments attach to the surface. When this occurs, the total system will gain less energy ($\chi_{sB} < \chi_{sA}$) but at the same time lose less entropy as compared to the adsorption of additional free block copolymer. In both scenarios the free energy of the system will decrease, and the competition between the two mechanisms is determined by a subtle balance involving the difference in segmental adsorption energy of A and B and the relative lengths of the blocks. When the difference decreases, relatively more B segments adsorb. As a consequence, the adsorbed amount decreases for almost all polymer compositions when the adsorption energy of B increases (but remains below that of A). Only at very low ν_A , below a crossover point in the *buoy regime*, does the adsorption increase, but it is relatively low in this region. The more weakly adsorbing B blocks must be long enough to compete with the A blocks for adsorbing sites. Decreasing the difference in segmental adsorption energy will decrease the necessity of a relatively long B block and therefore the maximum shifts to a higher ν_A , in other words to a shorter B block. The maximum disappears when the difference is zero ($\chi_{sA} = \chi_{sB}$).

We conclude that for small differences in adsorption energy the maximum is found at a composition where the A block is longer than the B block. However, the theoretical maximum is not as pronounced as the one we found experimentally. To investigate whether we can find a better qualitative agreement, we consider the influence of the solvency parameters (i.e., χ_{AO} and χ_{BO}) and of the block (in)compatibility (i.e., χ_{AB}).

In Figure 10 we give some results for a block copolymer with a small difference in segmental adsorption energy between the blocks ($\chi_{sA} = 2kT$, $\chi_{sB} = 1.87kT$).

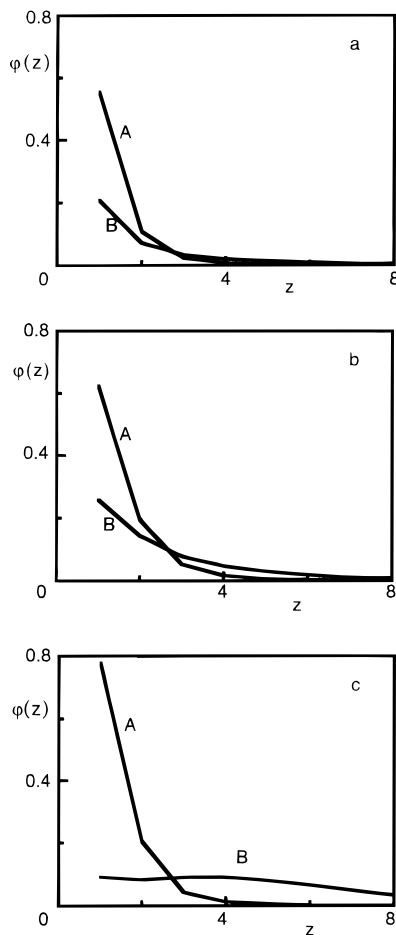


Figure 11. Volume fraction profiles ($\varphi(z)$) of the A and B blocks at the maximum value of θ^* in Figure 10.

When we choose a positive interaction energy between the segments and the solvent ($\chi_{AO} = \chi_{BO} = 0.45$, curve b), the adsorbed amount is increased for all compositions of the block copolymer as compared to the adsorption from an athermal solvent (curve a). To reduce the amount of unfavorable polymer-solvent contacts, the solvent is expelled from the adsorbed layer. The lateral repulsion between the polymers is reduced and more chains can adsorb per unit area. The layer is more compact as compared to a layer adsorbed from an athermal solution. This can also be seen in the volume fraction profiles of the A and B blocks in the adsorbed layer for the two different solvencies (parts a and b of Figures 11). These volume fraction profiles are given for compositions that give a maximum in Figure 10. In Figure 11a, most segments of both blocks can be found in the first few layers close to the surface. Nevertheless, a small segregation can be seen as the B segments are relatively more extended in the solution than the A segments. In Figure 11b the fraction of A and B segments in the first layers is enhanced because the solvent is expelled from the adsorbed layer due to the repulsive interaction between the polymer segments and the solvent. The segregation between A and B segments, necessary for an anchor-buoy structure of the adsorbed layer, is evolving: the B layer is slightly more extended into the solution than in Figure 11a.

When the solvent quality decreases, less anchoring segments are needed to keep the whole polymer attached to the surface in comparison with an athermal solution, which causes a shift in the position of the

maximum to a slightly lower ν_A and a slight increase in the relative height of the maximum (defined as the ratio between the adsorbed amounts in the maximum and at $\nu_A = 1$). These two effects due to the solvency (Figure 10) are, however, small in comparison to those occurring when the adsorption energies are varied (Figure 9).

When we assign a positive interaction energy to A-B contacts (i.e., the A and B blocks now become incompatible if they are long enough), the shape of the curve changes remarkably. The relative height of maximum is increased considerably, and a minimum appears at low ν_A . The minimum can be explained by considering the structure of the adsorbed layer. At low ν_A the A and B segments are forced to have many unfavorable contacts with each other in the mixed adsorbed layer; the total repulsive interaction energy is therefore high and the adsorption is decreased. The segregation, already seen in the volume fraction profiles in Figure 11b, is promoted by the incompatibility of the A and B blocks, so that the number of A-B contacts is further reduced. This effect is demonstrated in the volume fraction profiles of the A and B blocks given in Figure 11c. The first layer is almost completely occupied by adsorbed A segments, whereas most B segments form a more dilute buoy layer, extending away from the surface. A real anchor-buoy structure can be seen, although it is not as pronounced as in Figure 1b. The reason for this anchor-buoy structure is different from that in Figure 1b. In the latter case, it is the difference in adsorption energy; in Figure 11c, it is block incompatibility.

Statistically, the amount of unfavorable A-B contacts is the highest when both blocks are equal in size. For a block copolymer in which the A and B segments have the same segmental adsorption energy and a positive AB interaction energy, this gives rise to a minimum in the adsorbed amount as a function of the polymer composition at $\nu_A = 0.5$ (result not shown). When the A and B segments have a slightly different adsorption energy the minimum is shifted to $\nu_A < 0.5$ and a maximum develops at $\nu_A > 0.5$, as seen in Figure 10c. The theoretical curve in Figure 10c is in qualitative agreement with the experimental results presented in Figures 7 and 8. Experimentally we do not find a minimum, but the number of available compositions of the block copolymers was rather low; it would be interesting to include samples with ν_A around 0.3.

The calculations presented above were performed with equally flexible blocks. In reality, however, the chain stiffness might well be different. It is an established fact that some polymers are rather flexible, whereas others are stiff due to large side groups or internal structures. We performed some SCF calculations where we assigned a positive bending energy to one of the blocks or to both blocks, along the lines reported in the literature.¹ The effect of introducing chain stiffness appears to be very small and is definitely less pronounced than those of changing solvency and block incompatibility. The results of the theoretical calculations with stiff polymers are therefore not shown here.

Conclusions

The adsorption of two series of block copolymers and the corresponding homopolymers on silica was measured with reflectometry, and the hydrodynamic layer

thickness was determined by dynamic light scattering. All polymers adsorb by the same mechanism: hydrogen bonding between an oxygen of the polymer and a silanol group on the silica surface. The segmental adsorption energy is relatively high, of the order of $5kT$.³² On the other hand, the *difference* between the segmental adsorption energies of the two blocks is low, giving rise to nonselective adsorption of the block copolymers. For two types of block copolymers used in this study, the adsorbed amount as a function of block copolymer composition shows a shallow maximum; at this maximum, the longest block is also the strongest adsorbing block. The same trend is found for the hydrodynamic layer thickness. These findings differ from theoretical predictions concerning selective adsorption, where a pronounced maximum is found for a short anchor block.

With numerical self-consistent field calculations, we demonstrated that the same trends as in our experimental findings can be predicted by theory. In nonselective adsorption, when the difference between the adsorption energies of the blocks is low, both blocks compete for the same adsorption sites on the surface. When the differences in solvency are small and the blocks are compatible, only a very shallow maximum is seen at high fraction of A segments v_A . Assigning a positive interaction energy to the two different segments decreases the compatibility of the blocks. Due to this incompatibility, the blocks try to avoid each other, which promotes an anchor–buoy structure. This effect gives rise to a considerable increase of the adsorbed amount in the maximum as a function of the block copolymer composition. At this maximum, the longest block is also the strongest adsorbing block. For this nonselective adsorption with incompatible blocks the typical anchor–buoy structure of the adsorbed layer, necessary for an effective steric stabilization, is maintained, but it is less pronounced than for selective adsorption. The buoy layer is far less extended into the solution.

The nonselectively adsorbed block copolymers show a higher adsorbed amount and a higher hydrodynamic thickness as compared to the homopolymers of similar molar mass. Even though the effects are not as outspoken as found for selectively adsorbed block copolymers, this kind of block copolymer is promising for the steric stabilization of aqueous dispersions.

References and Notes

- (1) Fleer, G. J.; Cohen Stuart, M. A.; Scheutjens, J. M. H. M.; Cosgrove, T.; Vincent, B. *Polymers at Interfaces*, Chapman & Hall: London, 1993.
- (2) Kawaguchi, M.; Takahashi, A. *Adv. Colloid Interface Sci.* **1992**, *37*, 219.
- (3) Marques, C. M.; Joanny, J. F. *Macromolecules* **1989**, *22*, 1454.
- (4) Munch, M. R.; Gast, A. P. *Macromolecules* **1988**, *21*, 1366.
- (5) Evers, O. A.; Scheutjens, J. M. H. M.; Fleer, G. J. *J. Chem. Soc., Faraday Trans.* **1990**, *86*, 1333.
- (6) Wu, D. T.; Yokoyama, A.; Setterquist, R. L. *Polym. J.* **1991**, *23*, 711.
- (7) Cosgrove, T.; Phipps, J. S.; Heath, T. G.; Richardson, R. M. *Macromolecules* **1991**, *24*, 94.
- (8) Parsonage, E.; Tirrell, M.; Watanabe, H.; Nuzzo, R. G. *Macromolecules* **1991**, *24*, 1987.
- (9) Guzonas, D. A.; Boils, D.; Tripp, C. P.; Hair, M. L. *Macromolecules* **1992**, *25*, 2434.
- (10) Guzonas, D.; Hair, M. L.; Cosgrove, T. *Macromolecules* **1992**, *25*, 2777.
- (11) Webber, R. M.; Anderson, J. L. *Langmuir* **1994**, *10*, 3156.
- (12) Halperin, A.; Tirell, M.; Lodge, T. P. *Adv. Polymer Sci.* **1992**, *100*, 31.
- (13) Fleer, G. J.; Scheutjens, J. M. H. M. *Colloids Surf.* **1990**, *51*, 281.
- (14) Marques, C. M.; Joanny, J. F.; Leibler, L. *Macromolecules* **1988**, *21*, 1051.
- (15) Van Lent, B.; Scheutjens, J. M. H. M. *Macromolecules* **1989**, *22*, 1931.
- (16) Malmsten, M.; Linse, P.; Cosgrove, T. *Macromolecules* **1992**, *25*, 2474.
- (17) Tiberg, F.; Malmsten, M.; Linse, P.; Lindman, B. *Langmuir* **1991**, *7*, 2723.
- (18) Munch, M. R.; Gast, A. P. *Macromolecules* **1990**, *23*, 2313.
- (19) Johner, A.; Joanny, J. F. *Macromolecules* **1990**, *26*, 5299.
- (20) Huguenard, C.; Varoqui, R.; Pefferkorn, E. *Macromolecules* **1991**, *24*, 2226.
- (21) Tripp, C. P.; Hair, M. L. *Langmuir* **1996**, *12*, 3952.
- (22) Liu, Q.; Konas, M.; Davis, R. M.; Riffle, J. S. *J. Polym. Sci., Part A—Polym. Chem.* **1993**, *31*, 1709.
- (23) Miyamoto, M.; Sano, Y.; Saegusa, T.; Kobayashi, S. *Eur. Polym. J.* **1983**, *19*, 955.
- (24) Brandrup, J.; Immergut, E. H., Eds. *Polymer Handbook*, 3rd ed.; Wiley and Sons: New York, 1989.
- (25) Van Krevelen, D. W. *Properties of Polymers, Their Estimation and Correlation with Chemical Structure*, Elsevier: Amsterdam, 1976.
- (26) De Vos, R. J.; Goethals, E. J. *Makromol. Chem., Rapid Commun.* **1985**, *6*, 53.
- (27) Dijt, J. C.; Cohen Stuart, M. A.; Hofman, J. E.; Fleer, G. J. *Colloids Interfaces* **1990**, *51*, 141.
- (28) Scheutjens, J. M. H. M.; Fleer, G. J. *J. Phys. Chem.* **1979**, *83*, 1619.
- (29) Scheutjens, J. M. H. M.; Fleer, G. J. *J. Phys. Chem.* **1980**, *84*, 178.
- (30) Gorbunov, A. A.; Zhulina, E. B.; Skvortsov, A. M. *Polymer* **1982**, *23*, 1133.
- (31) Van der Beek, G. P.; Cohen Stuart, M. A. *J. Phys. (Paris)* **1988**, *49*, 1449.
- (32) Chen, C. H.; Wilson, J. E.; Davis, R. M.; Chen, W.; Riffle, J. S. *Macromolecules* **1994**, *27*, 6376.

MA9618742